Pergamon

Tetrahedron 58 (2002) 799–805

TETRAHEDRON

Recognition-directed assembly of salt-binding [2]rotaxanes

Martin J. Deetz, Rameshwer Shukla and Bradley D. Smith*

Department of Chemistry and Biochemistry, University of Notre Dame, Notre Dame, IN 46556-5670, USA

Received 29 May 2001; revised 9 September 2001; accepted 10 September 2001

Abstract—This paper describes the synthesis of four isomeric [2]rotaxanes and includes the first example of a salt binding [2]rotaxane with the following key observations. In polar solvents the [2]rotaxane undergoes a relatively slow co-conformational exchange that produces broad signals in the ^{1}H NMR spectrum. Upon complexation with K^+, the NMR signals sharpen apparently because the rotaxane adopts a single co-conformation. In contrast, the binding of Cl^- has no effect on the rotaxane's dynamic behavior. Although the binding of K^+ induces a preorganization of the [2]rotaxane it does not change the rotaxane/Cl^- association constant. The paper finishes with a discussion of the future directions of this work. © 2002 Elsevier Science Ltd. All rights reserved.

1. Introduction

A [2]rotaxane is an interlocked molecule in which a macrocyclic wheel is threaded onto an acyclic dumbell-shaped axle. The ends of the axle have stopper groups that are large enough to prevent dissociation of the components, i.e. the components are held by a mechanical bond. The past decade has seen a renaissance in rotaxane chemistry after the initial investigations more than 30 years ago.[1] In recent years, a range of exotic rotaxane structures has been prepared, and a number of new synthetic strategies have been developed.[2–7] The modern strategies rely on recognition-directed methods to template the rotaxane forming reaction. Currently, three main methods are employed for rotaxane assembly (Fig. 1). (a) *Clipping* is when a macrocycle is assembled around the dumbell-shaped axle,[8] (b) *Threading* involves binding of an unstoppered axle within a macrocycle (this complex is sometimes referred to as a *psuedorotaxane*) followed by an axle-capping reaction that traps the components together,[9] and (c) *Slipping* involves mechanical slippage of a macrocycle over the dumbell-shaped axle.[10]

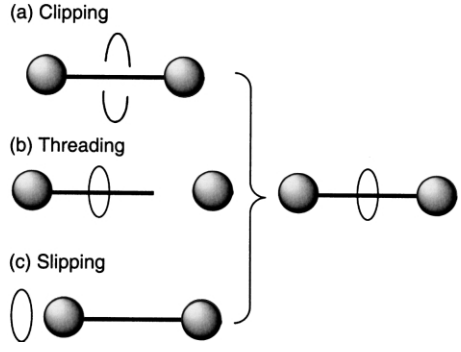

Figure 1. Three recognition-directed methods for assembling [2]rotaxanes.

Recently, Vögtle and coworkers reported a new threading method that employs an anion trapping effect.[11–13] The example shown in Fig. 2 uses a macrocyclic tetralactam to bind a bulky phenolate anion via hydrogen bonding to its isophthalamide NH protons.[11,12] This complex then functions as a *wheeled supramolecular nucleophile*, and reacts with an electrophile through the cavity of the macrocycle to form a *semiaxle*. Dissociation of the components, followed by reaction of the semiaxle with a second wheeled phenolate produces the [2]rotaxane. Yields of up to 95% have been obtained using this trapping method,[11] although more often the yields are below 50%.[12] It should be noted that 18-crown-6 is a crucial additive to this reaction, as it increases the solubility of the K_2CO_3 base and most likely prevents the formation of a tight ion pair between the potassium and the phenolate.[12] A tight ion pair reduces phenolate reactivity

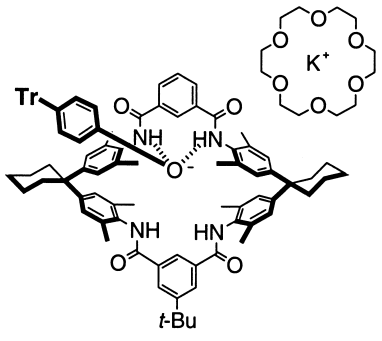

Figure 2. Vögtle's wheeled phenolate, Tr=Trityl.[11,12]

Keywords: interlocked molecule; supramolecular chemistry; molecular machine; anion binding.

* Corresponding author. Tel.: +1-219-631-8632; fax: +1-219-631-6652; e-mail: smith.115@nd.edu

PII: S0040-4020(01)01108-5

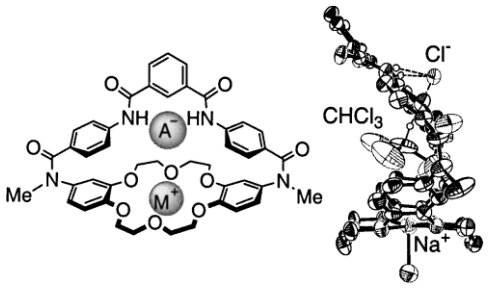

Figure 3. Left: salt-binding macrobicycle. Right: side-view of the X-ray crystal structure of $Na^+ \cdot CHCl_3 \cdot Cl^-$ complex.

and also inhibits binding of the phenolate to the macrocyclic wheel.

Our group has become interested in this anion trapping reaction for the following reasons. Recently, we prepared a number of macrobicyclic receptors and demonstrated that they can simultaneously bind a cation and an anion.[14,15] One example is the macrobicyclic receptor shown in Fig. 3 which binds sodium chloride as a solvent separated ion-pair.[15] The anion forms hydrogen bonds to the exo-face of the isophthalamide bridge, and the cation is encapsulated within the ring of the crown ether. This supramolecular structure prompted us to consider whether the anion template reaction could be used to convert our salt-binding macrobicycle into a novel [2]rotaxanes with the generic structure shown in Fig. 4. The interesting feature with our system is that the crown ether required for the reaction to proceed is now part of the rotaxane wheel. Moreover, because the resulting [2]rotaxane has a crown ether incorporated into its wheel component, the rotaxane is likely to have interesting supramolecular properties. Recently, we communicated our first discovery in this fascinating field of interlocked molecules,[16] and in this paper we describe our work in more detail. Specifically, we describe the

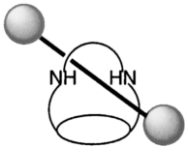

Figure 4. [2]Rotaxane with bicyclic wheel.

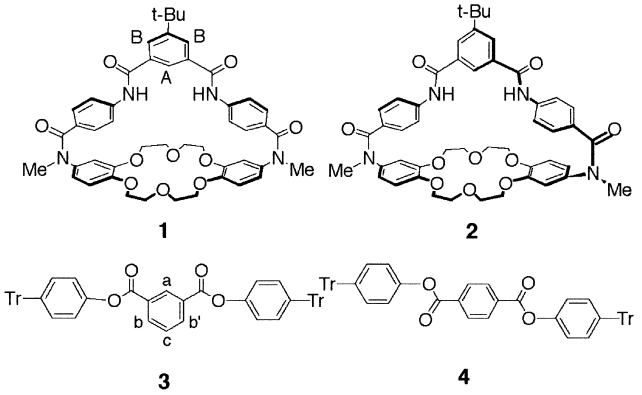

Figure 5. Isomeric wheel components **1** and **2** and axle components **3** and **4**, Tr=Trityl.

syntheses of four isomeric [2]rotaxanes that use bicycles **1** and **2** as wheel components and phthalate diesters **3** and **4** as axle components (Fig. 5).

2. Results and discussion

The syntheses of isomeric salt-binding macrobicycles **1** and **2** are outlined in Scheme 1. The synthetic scheme has already been reported for the *cis* isomer, **1**,[15] and so it is not discussed here, except to state that compounds **1** and **2** can be prepared on a gram scale in six steps from dibenzo-18-crown-6, and that mass spectra of the crude products of the final macrocyclization reactions show no evidence for larger polycyclic structures. The X-ray crystal structure of trans isomer, **2** (Fig. 6) shows that it has pseudo-C_2 symmetry and a slightly smaller cavity than the *cis* isomer **1**.

In solution, macrobicycles **1** and **2** bind salts with positive cooperativity, i.e. the presence of a metal cation enhances anion affinity. Association constants were determined using standard NMR titration methods. Solutions of **1** and **2** in DMSO-d_6/CD_3CN (3:1) were titrated with tetrabutylammonium chloride in the presence and absence of 1 molar equiv. of potassium tetraphenylborate and the resulting titration isotherms fitted to a 1:1 binding model using established iterative curve fitting methods.[17] As shown in Table 1, *cis* isomer **1** has 2.5 times higher Cl^- affinity than trans isomer **2**. In each case the Cl^- association

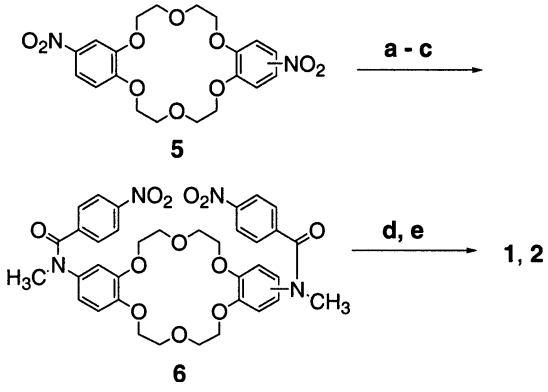

Scheme 1. *Reagents and conditions*: (a) H_2 (30 psi), Pd–C, DMF, *cis*—98%, (*trans*—99%), (b) 4-nitrobenzoyl chloride, Et_3N, CH_2Cl_2, *cis*—99% (*trans*—99%), (c) NaH, CH_3I, DMF, *cis*—99% (*trans*—96%), (d) Fe (powder), HCl, *cis*—81% (*trans*—77%), (e) corresponding isophthaloyl dichloride, Et_3N, CH_2Cl_2, *cis*—32–75% (*trans*—42–45%).

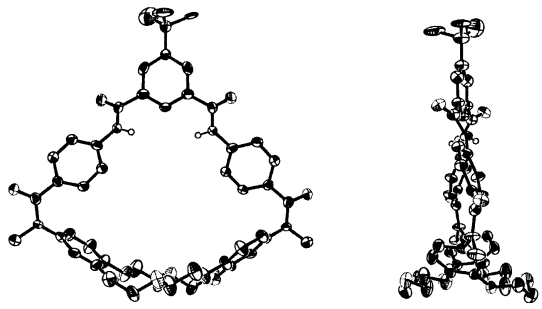

Figure 6. Front and side views of the X-ray crystal structure of macrobicycle **2**.

Table 1. Receptor/Cl^- association constants (K_{Cl^-}) and change in NH chemical shift ($\Delta\delta_{max}$)

	1	**1**+K^{+a}	**2**	**2**+K^{+a}	[**1**·**3**]	[**1**·**3**]+K^{+a}
K_{Cl^-} (M^{-1})[b]	50	350	20	130	300	300
$\Delta\delta_{max}$ (ppm)[c]	0.60	0.92	0.50	0.84	0.96	1.19

[a] Presence of 1 molar equiv. of $KBPh_4$.
[b] Uncertainty ±20%, T=295 K, [Receptor]=10 mM in DMSO-d_6/CD_3CN (3:1).
[c] $\Delta\delta_{max}$ represents the change in NH chemical shift after addition of 4 molar equiv. of $N(Bu_4)Cl$.

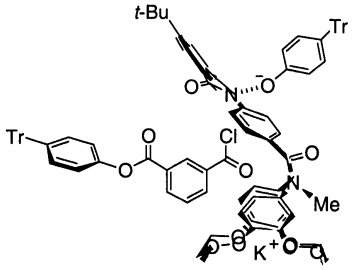

Figure 7. Reaction of wheeled phenolate to give semiaxle **7** and subsequently [2]rotaxane [**1**·**3**], Tr=Trityl.

constants are increased by about a factor of seven when the titration is repeated in the presence of 1 molar equiv. of potassium tetraphenylborate.

A diagram of the proposed trapping effect is shown in Fig. 7. We expected that **1** would be able to bind potassium 4-trityl-phenolate as its solvent separated pair. Reaction of the wheeled potassium phenolate with isophthaloyl dichloride, for example, first forms semiaxle **7** in situ and subsequently the [2]rotaxane, [**1**·**3**]. While the anion templated esterification method employed by Vögtle and coworkers requires non-polar solvents to ensure high amounts of wheeled nucleophile, our procedure produces [2]rotaxanes in a range of organic solvents such as chloroform, THF, and even THF–DMF. With the former two solvents, the reaction is hampered by precipitation of a macrobicycle/KCl complex. Changing to the more polar mixture of THF/DMF produces homogeneous solutions, faster reaction times, and slightly better yields. The most efficient procedure mixes the macrobicycle, and potassium trityl phenolate (2 molar equiv.) at 0°C for 10–15 min in a 5/1 mixture of THF and DMF, followed by single addition of all of the appropriate solid phthaloyl dichloride. The reaction mixture is slowly warmed to room temperature and then stirred under an inert atmosphere for 2–3 days. The [2]rotaxanes are produced in 3–20% yield after chromatography (Table 2). Although the yields are low, it should be remembered that two covalent bonds are formed and four units are assembled in a single reaction. The [2]rotaxanes from *cis* macrobicycle, **1**, are produced in higher yields than *trans* macrobicycle, **2**. The difference likely stems from a more productive preorganization of the axle components within the larger *cis* macrobicyclic cavity. The reaction fails to produce [**1**·**3**] when cesium or tetrabutylammonium 4-tritylphenolate is used. The dibenzocrown unit in **1** is known to have a low affinity for large and diffuse cations,[18] so we consider this observation as evidence in favor of the templating model shown in Fig. 7. The size of the stopper groups appears to be important because no [2]rotaxane is isolated when the less spatially demanding 3,5-di-*t*-butyl phenol, is used.[10]

Table 2.

[2]Rotaxane		Isolated yield (%)
Wheel	Axle	
1	**3**	20
1	**4**	17
2	**3**	6
2	**4**	3

The structures of the [2]rotaxanes were proven by mass spectrometry and NMR spectroscopy. Positive ion FAB mass spectra of the isomeric [2]rotaxanes show a weak or non-existent molecular ion signal at *m*/*z* 1647 $[M+H]^+$, and intense signals at 1669 $[M+Na]^+$ and 1685 $[M+K]^+$ due to complexation with adventitious cations in the sample matrix. Rotaxane formation is readily indicated by the changes in the ^1H NMR signals for the axle phathalate protons. The signal for the two isophthalate protons, H_b, in axle **3** is a doublet at 8.43 ppm when free in $CDCl_3$ solution, but when incorporated into [2]rotaxane [**1**·**3**], the two protons are no longer chemically equivalent and two doublets at 8.64 and 8.55 ppm are observed. With [2]rotaxane [**2**·**3**], the two protons are chemically equivalent due to the C_2 symmetry of the wheel and only one doublet is observed at 8.43 ppm. The signal for the four terephthalate protons in axle **4** is a singlet at 8.04 ppm, when free in $CDCl_3$ solution, but when incorporated into [2]rotaxane [**1**·**4**], two doublets are observed at 8.53 and 8.41 ppm. In the case of [2]rotaxane [**2**·**4**], a single peak is observed at 8.40 ppm.

The room temperature ^1H NMR spectra of all [2]rotaxanes in $CDCl_3$ are well resolved and exhibit no apparent dynamic behavior upon cooling to −60°C. In the case of [**1**·**3**], the spectrum was assigned by COSY and ROESY NMR methods. The ROESY spectrum is consistent with the co-conformation (the relative orientation of the component parts of an interlocked molecule has been defined as its co-conformation[19]) shown in Fig. 8. For example, the axle proton H_a (8.92 ppm) interacts through-space with the wheel NH residues (8.18 ppm) and proton H_A (7.74 ppm), there are also cross peaks between axle protons H_b (8.54, 8.64 ppm), H_c (8.12 ppm) and the wheel's crown ether protons (3.4–4.2 ppm).

In the more polar solvents, DMSO-d_6 and acetone-d_6, the

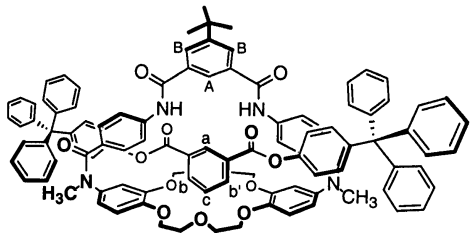

Figure 8. Likely co-conformation of [**1**·**3**] in $CDCl_3$.

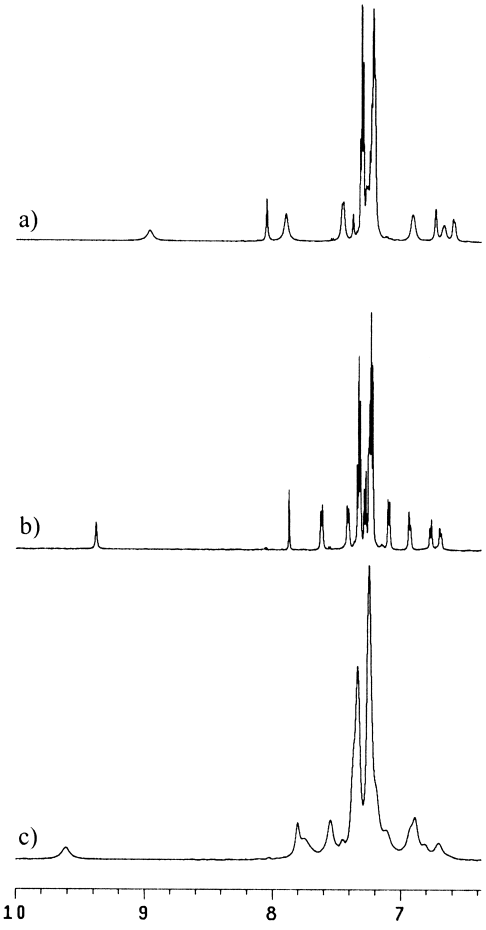

Figure 9. ^{1}H NMR spectra of [2]rotaxane [**2·4**] in acetone-d_6 at: (a) +20°C, (b) −40°C, and (c) −90°C.

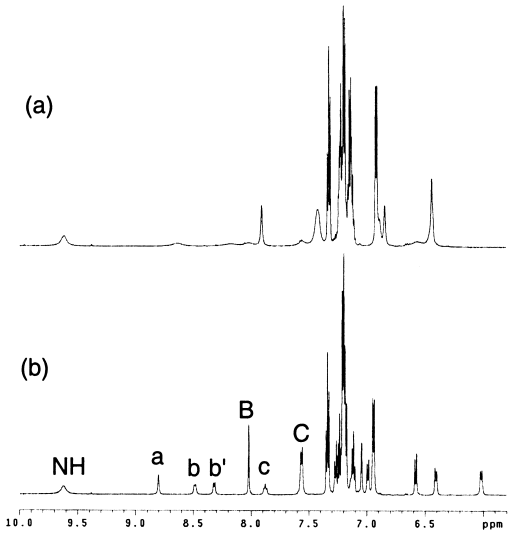

Figure 10. Partial ^{1}H NMR spectra of [2]rotaxane [**1·3**] in DMSO-d_6: (a) before and (b) after the addition of 5 molar equiv. of KPF_6.

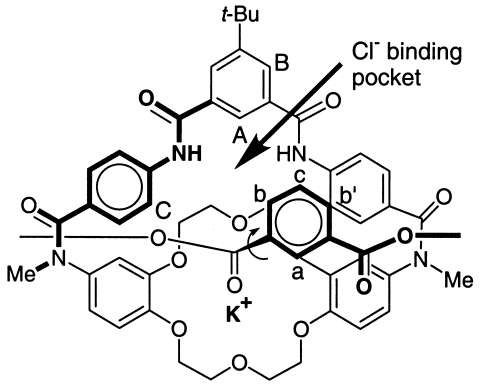

Figure 11. Likely supramolecular structure of the [**1·3**]/K^+ complex. The curved arrow indicates rapid bond rotation in the absence of Cl^-.

NMR spectra are broad at room temperature. Cooling the acetone-d_6 samples to −40°C results in increased spectrum resolution, but only one set of peaks is observed. Further cooling to −90°C leads to signal broadening. The three spectra of [2]rotaxane [**2·4**] shown in Fig. 9, are typical examples. The lack of peak splitting makes it hard to attribute the peak broadness at room temperature to a specific dynamic motion. The two most likely motions are pirouetting of the wheel around the axle and shuttling of the wheel along the axle.[20]

The broad NMR spectrum of [**1·3**] in DMSO-d_6 sharpens considerably upon addition of 5 molar equiv. of KPF_6 at room temperature (Fig. 10). There are two possible explanations for this observation: either the added K^+ increases the rate of exchange between different co-conformations of [**1·3**], or the K^+ freezes out a single co-conformation.[20] Evidence for the latter explanation is gained from the ROESY spectrum of [**1·3**] in DMSO-d_6 with added KPF_6 which is consistent with a predominant co-conformation. For example, the wheel's crown ether protons cross-relaxes the axle protons H_a and H_b but not protons $H_{b'}$ and H_c. It appears that the potassium cation binds to the benzocrown ring and freezes out a single rotaxane co-conformation by coordinating to one of the ester carbonyls in the axle (Fig. 11). A CPK model of [**1·3**] indicates that this co-conformation allows rapid rotation about the carbonyl–phenyl bond which interchanges the spatial positions of H_a and H_b so they pass close to the crown hydrogens, whereas $H_{b'}$ and H_c always remain more than 4 Å from the crown. Further evidence for this supramolecular structure is provided in the next paragraph.

The anion and salt binding properties of [2]rotaxane [**1·3**] were evaluated in the following way. First, a solution of [**1·3**] in DMSO-d_6/CD_3CN (3:1) was titrated with $N(Bu_4)Cl$. The NMR signals for [**1·3**] remained broad throughout the titration, although the NH peak could always be identified. The change in NH chemical shift was monitored and used to generate a titration isotherm which was fitted to 1:1 binding model using an iterative computer method.[17] The titration experiment was then repeated but this time the host solution also included 1 molar equiv. of $KBPh_4$ which sharpens the ^{1}H NMR spectrum of [**1·3**]. The changes in rotaxane chemical shifts ($\Delta\delta$) for [**1·3**]/$KBPh_4$ induced by the addition of 4 molar equiv. of tetrabutylammonium chloride are listed in Table 3. The large $\Delta\delta$ values observed for H_A, H_C, NH, H_b and H_c are strong evidence that the Cl^- ion binds in a pocket formed by these hydrogens. The small $\Delta\delta$ value observed for H_a

Table 3. Change in ^{1}H NMR chemical shifts ($\Delta\delta_{max}$) for [**1**·**3**]/$KBPh_4$ upon addition of $N(Bu_4)Cl$

Signals[a]	NH	H_a	H_b	$H_{b'}$	H_c	H_A	H_B	H_C
$\Delta\delta_{max}$ (ppm)	1.19	0.04	0.33	−0.03	−0.22	0.65	−0.05	0.29

Final molar ratio of [**1**·**3**]/$KBPh_4$/$N(Bu_4)Cl$ was 1:1:4 in DMSO-d_6/CD_3CN (3:1).
[a] See Fig. 5 for hydrogen labeling scheme.

indicates that carbonyl–phenyl rotation is restricted upon binding of KCl, and that H_a points away from the Cl^- binding pocket. Overall, the data agrees nicely with the supramolecular structure shown in Fig. 11.

Table 1 compares the [**1**·**3**]/Cl^- and **1**/Cl^- association constants in the presence and absence of 1 molar equiv. of $KBPh_4$. Inspection of the association constants reveals some surprising effects. First, in the absence of K^+ ions, macrobicycle **1** has a six-fold lower Cl^- affinity than [2]rotaxane [**1**·**3**] in DMSO-d_6/CD_3CN (3:1). The large changes in NH chemical shift clearly indicate that in both cases the NH residues form hydrogen bonds to the Cl^-. It is known from our previous work that a DMSO solvent molecule binds deeply within the cavity of macrobicycle **1**, and thus it competes strongly with the Cl^-.[15] In the case of [2]rotaxane [**1**·**3**], a DMSO molecule cannot bind to the macrobicyclic wheel in the same ditopic fashion, and does not appear to strongly inhibit Cl^- binding to the wheel NH protons. In the presence of 1 molar equiv. of $KBPh_4$ the **1**/Cl^- affinity was enhanced seven-fold, whereas the presence of $KBPh_4$ had no effect on [**1**·**3**]/Cl^- affinity. The fact that no binding enhancement is observed in the rotaxane case indicates that the axle is insulating any through-space electrostatic interaction between the bound K^+ and Cl^-. This is in contrast to a recently proposed induced-dipole model that predicts electrostatic stabilizing effects can be transmitted through aromatic groups.[21] It seems that in this present case the orientation of the central phthalate ring in the axle does not allow such a π-cloud polarization effect to occur.

3. Conclusions

This paper describes the first example of a salt binding [2]rotaxane and includes the following key observations. In polar solvents the [2]rotaxane [**1**·**3**] undergoes a relatively slow co-conformational exchange that produces broad signals in the ^{1}H NMR spectrum. Upon complexation with K^+, the NMR signals sharpen apparently because the rotaxane adopts a single co-conformation. In contrast, the binding of Cl^- has no apparent effect on the dynamic behavior of [2]rotaxane [**1**·**3**], however, the combined effect of KCl produces the most structural rigidity. Although the binding of K^+ induces a preorganization of [2]rotaxane [**1**·**3**] it does not change the [**1**·**3**]/Cl^- association constant. A schematic model of the proposed conformational and binding equilibria is provided in Fig. 12.

It appears that Vögtle's anion trapping method will be a versatile recognition-directed approach to assembling interlocked molecules.[11–13] The results of this study indicate that

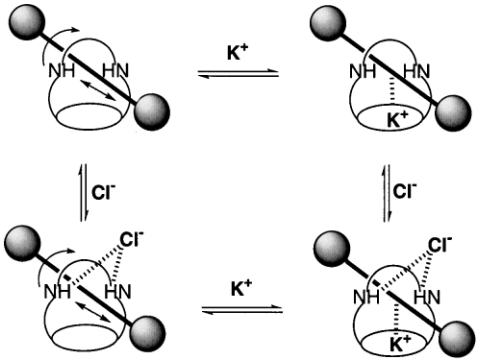

Figure 12. In polar aprotic solvent, the [2]rotaxane [**1**·**3**] populates multiple axle/wheel orientations. Binding Cl^- does not measurably alter the rotaxane's dynamic properties whereas binding K^+ freezes out a single co-conformation, and the combined effect of KCl produces the most structural rigidity.

the anion trapping reaction can be used to prepare salt binding rotaxanes and that these molecules have the potential to exhibit chemical-dependent dynamic behavior. To date, most attempts to control the motion of rotaxane and catenanes have used photochemical or electrochemical strategies.[22,23] Such designs are attractive because light and redox potential are readily amenable to spatiotemporal control. Thus, it is not surprising that these systems are being considered as components in light harvesting[24] and logic devices.[25] The relatively few reports of chemical switching of interlocked co-conformation include the use of protons,[22,23,26] metal cations,[19,27–29] anions[30,31] and amines[32] as chemical effectors. In these cases, the potential applications include sensing, separations, catalysis and drug delivery, although few working prototypes have appeared so far. A lingering technological hurdle is the need for efficient syntheses of interlocked compounds.[2] Although the last decade has seen remarkable advances in recognition-directed synthesis, most of the presently accessible interlocked molecules, such as the [2]rotaxane [**1**·**3**] described here, are still relatively simple structures when compared to the molecular machines found in nature.[22,23] In particular, the development of high yielding, iterative synthetic methods that can rapidly build sophisticated polyrotaxanes and polycatenanes would undoubtedly bring major advances to the field.[33,34] Of course a related technical issue is the development of analytical methods to characterize these larger and more complicated molecular structures.[20] The ongoing improvements in molecular imaging will definitely help in this regard.[35]

From a broader perspective, the work described in this paper can be viewed as a step towards the development of *artificial molecular machines* although some may consider such a claim as hyperbole.[36] As a compromise we state that our near-term research goals are to invent molecular versions of *machine elements* which have been defined as "One of the various simple mechanisms, as the lever, pulley, cam, gear-wheel, etc. which, alone or in combination, facilitate conversion of energy to useful work".[37] The phrase 'conversion of energy to useful work' is a critical point and needs to be emphasized. Although certain applications such as catalysis and drug delivery can be achieved in homogeneous solution, many others will require the molecular

machine elements to be assembled and employed in a coherent manner. Thus, the challenge for researchers is to align them in ordered arrays on surface or interfaces, so that their individual molecular outputs can be combined and amplified to produce a measurable macroscopic output.

4. Experimental

4.1. Materials

All salts and NMR solvents were purchased from Aldrich and, after checking for purity, were used as supplied.

4.1.1. Macrobicycles 1 and 2. The synthesis of *cis* isomer **1** from dibenzo18-crown-6 has been reported elsewhere in detail.[15] The same procedure was used to make the *trans* isomer **2**. ^{1}H NMR (300 MHz, $CDCl_3$) δ (ppm) 8.31 (bs, 2H), 8.17 (s, 2H), 7.80 (s, 1H), 7.39 (d, 4H, J=8.4 Hz), 7.22 (d, 4H, J=8.6 Hz), 6.64 (d, 2H, J=8.4 Hz), 6.52 (d, 2H, J=8.2 Hz), 6.47 (s, 1H), 4.09–3.79 (m, 16H), 3.34 (s, 6H), 1.39 (s, 9H) ppm. ^{13}C NMR (75 MHz, DMSO-d_6) δ (ppm) 170.0, 165.5, 153.5, 148.7, 147.1, 139.3, 138.2, 134.9, 131.1, 129.7, 129.1, 121.2, 119.5, 119.0, 111.7, 111.0, 69.6, 69.6, 67.8, 38.6, 35.2, 31.2. MS (FAB^+) exact mass calculated for $C_{48}H_{51}N_4O_{10}$ $[M+H]^+$ 843.3605, found 843.3594. X-Ray crystal data were collected and integrated using a Bruker Apex system, with graphite monochromated Mo Kα (λ=0.71073 Å) radiation at 170 K. The structure was solved by direct methods. Hydrogen atoms were placed at idealized positions and a riding model with fixed thermal parameters was used for subsequent refinements. The asymmetric unit contains one half of the macrocycle, with one orientation of the *t*-butyl methyl groups at 50% occupancy. The second orientation of the *t*-butyl methyl groups is generated through symmetry. The X-ray data has been deposited with the Cambridge Crystallographic Data Centre as supplementary publication number CCDC 168432. Copies of the data can be obtained free of charge on application to CCDC at deposit@ccdc.cam.ac.uk.

4.1.2. General rotaxane synthesis. Under an atmosphere of argon, macrobicycle **1** or **2** (0.025 g, 0.029 mmol) and potassium 4-tritylphenolate (0.022 g, 0.058 mmol) were stirred in 5:1 THF/DMF (18 mL) for 1 h. The solution was cooled to ice temperature then solid phthalolyl or isophthalolyl dichloride (0.006 g, 0.029 mmol) was added and the solution allowed to warm and stir for four days. The solvent was evaporated and the residue purified by column chromatography using silica gel and CH_2Cl_2/MeOH (95:5).

4.1.3. Rotaxane [1·3]. Yield 20%. ^{1}H NMR ($CDCl_3$, 600 MHz): δ (ppm) 8.92 (s, 1H), 8.64 (d, 1H, J=8.0 Hz), 8.55 (d, 1H, J=8.0 Hz), 8.24 (s, 2H), 8.17 (s, 2H), 8.12 (t, 1H, J=8.0 Hz), 7.72 (s, 1H), 7.23–7.06 (m, 40H), 6.96 (d, 2H, J=9.0 Hz), 6.75 (d, 2H, J=9.0 Hz) 6.48 (s, dd, 2H, J=8.5, 2.5 Hz), 6.35 (d, 2H, J=8.5 Hz), 6.14 (d, 2H, J=8.5 Hz), 4.05–4.03 (m, 4H), 3.80 (m, 6H), 3.68 (m, 2H), 3.52 (m, 2H), 3.42 (m, 2H), 3.35 (s, 6H), 1.34 (s, 9H). ^{13}C NMR ($CDCl_3$, 150 MHz): δ (ppm) 170.3, 167.6, 165.8, 164.8, 153.8, 148.5, 148.3, 148.0, 147.6, 147.2, 146.5, 146.5, 145.7, 145.5, 139.4, 138.3, 136.3, 136.2, 134.8, 132.5, 132.4, 132.2, 132.0, 131.5, 131.4, 131.3, 131.2, 131.1, 130.9, 130.1, 129.7, 129.6, 129.3, 127.9, 127.5, 126.2, 126.1, 126.0, 120.9, 120.5, 120.3, 118.8, 114.4, 112.9, 112.3, 70.1, 69.2, 69.0, 68.1, 64.7, 64.7, 38.9, 35.4, 31.2, MS (FAB^+) mass calcd for $C_{106}H_{92}N_4NaO_{14}$ $[M+Na]^+$ 1669, found 1669.

4.1.4. Rotaxane [1·4]. Yield 17%. ^{1}H NMR ($CDCl_3$, 300 MHz): δ (ppm) 8.53 (d, 2H, J=8.4 Hz), 8.41 (d, 2H, J=8.4 Hz), 8.30 (d, 2H, J=1.5 Hz), 8.13 (s, 2H), 7.68 (s (br), 1H), 7.29 (m, 40H), 6.57 (d, 2H, J=2.1 Hz), 6.44 (d, 2H, J=8.4 Hz), 6.01 (d, 2H, J=9.0 Hz) 4.09 (m, 4H), 3.93 (m, 4H), 3.65 (m, 4H), 3.45 (m, 2H), 3.37 (s, 6H), 3.30 (m, 2H), 1.30 (s, 9H). ^{13}C NMR ($CDCl_3$, 75 MHz): δ (ppm) 170.9, 168.6, 164.6, 153.9, 148.8, 147.9, 146.6, 146.5, 146.1, 145.5, 139.2, 138.3, 135.0, 135.0, 134.7, 132.8, 132.6, 132.5, 132.2, 131.3, 131.2, 130.8, 129.8, 129.3, 127.8, 127.6, 126.3, 126.2, 121.6, 120.5, 120.2, 119.9, 118.7, 113.5, 112.6, 70.4, 69.5, 69.0, 68.3, 64.8, 38.5, 35.4, 31.3 MS (FAB^+) mass calcd for $C_{106}H_{92}N_4NaO_{14}$ $[M+Na]^+$ 1669, found 1669.

4.1.5. Rotaxane [2·3]. Yield 6%. ^{1}H NMR (600 MHz, $CDCl_3$) δ (ppm) 8.90 (s, 1H), 8.43 (dd, 2H, J=1.7, 7.9 Hz), 8.27 (s, 2H), 8.12 (t, 1H, J=7.8 Hz), 8.13 (s, 2H), 7.62 (s, 1H), 7.26–7.11 (m, 42H), 6.46 (d, 4H, J=8.8 Hz), 6.43 (dd, 2H, J=2.4, 8.4 Hz), 6.40 (d, 2H, J=2.4 Hz), 6.30 (d, 2H, J=8.4 Hz), 4.00–3.37 (m, 16H), 3.38 (s, 6H), 1.33 (s, 9H) ppm. ^{13}C NMR (125 MHz, $CDCl_3$) (ppm) 169.6, 166.5, 164.7, 153.7, 148.7, 147.9, 146.9, 146.3, 145.7, 139.4, 138.4, 135.7, 134.6, 132.0, 131.6, 131.3, 130.9, 130.7, 129.8, 129.6, 129.5, 127.6, 126.0, 120.4, 119.9, 119.5. 118.5, 112.7, 111.8, 69.6, 69.4, 68.7, 68.1, 64.6, 38.6, 35.2, 31.1. MS (FAB^+) mass calculated for $C_{106}H_{92}N_4NaO_{14}$ $[M+Na]^+$, 1669, found 1669.

4.1.6. Rotaxane [2·4]. Yield 3%. ^{1}H NMR (600 MHz, $CDCl_3$) δ (ppm) 8.40 (s, 4H), 8.30 (d, 2H, J=1.4 Hz), 8.12 (s, 2H), 7.57 (s, 1H), 7.23–7.12 (m, 40H), 6.51 (d, 4H, J=8.8 Hz), 6.42 (dd, 2H, J=2.5, 8.4 Hz), 6.39 (d, 2H, J=2.5 Hz), 6.26 (d, 2H, J=8.4 Hz), 3.93–3.89 (m, 4H), 3.83 (dt, 2H, J=3.1, 9.5 Hz), 3.75 (td, 2H, J=2.3, 9.3 Hz), 3.66 (dt, 2H, J=2.9, 10.4 Hz), 3.58 (dt, 2H, J=2.7, 9.8 Hz), 3.49 (dt, 2H, J=2.9, 11.1 Hz), 3.35–3.32 (m, 2H), 3.38 (s, 6H), 1.34 (s, 9H) ppm. ^{13}C NMR (125 MHz, $CDCl_3$) δ (ppm) 169.7, 166.9, 164.6, 153.8, 148.6, 148.0, 146.9, 146.4, 145.9, 139.4, 138.1, 134.5, 133.4, 132.0, 131.8, 130.9, 130.7, 129.8, 129.7, 127.7, 126.0, 120.5, 119.7, 119.3, 118.4, 112.1, 111.6, 69.4, 69.3, 68.6, 67.8, 64.7, 38.5, 35.2, 31.0. MS (FAB^+) mass calculated for $C_{106}H_{92}N_4NaO_{14}$ $[M+Na]^+$, 1669, found 1669.

4.2. NMR titration experiments

Aliquots of tetrabutylammonium chloride stock solution were added to a 10 mM solution (3:1 DMSO-d_6/CD_3CN, 0.75 mL) of receptor in the presence and absence of potassium tetraphenylborate. The changes in receptor chemical shift were monitored and used to produce titration isotherms which were fitted to a 1:1 binding model using an iterative computer method that has been described elsewhere.[17]

Acknowledgements

This work was supported by the National Science Foundation and the University of Notre Dame (George M. Wolf and Reilly fellowships for M. J. D.). The X-ray structure of compound **2** was solved by Dr A. Beatty, University of Notre Dame.

References

1. Schill, G. *Catenanes, Rotaxanes, Knots*; Academic: New York, 1971.
2. *Molecular Catenanes, Rotaxanes and Knots*, Sauvage, J. P., Dietrich-Bucheker, C. O., Eds.; VCH-Wiley: Weinheim, 1999.
3. Leigh, D. A.; Murphy, A. *Chem. Ind.* **1999**, 178–184.
4. Reuter, C.; Schmieder, R.; Vögtle, F. *Pure Appl. Chem.* **2000**, *72*, 2233–2241.
5. Raymo, F.; Stoddart, J. F. *Chem. Rev.* **1999**, *99*, 1643–1663.
6. Bryant, W. S.; Guzei, I. A.; Reingold, A. L.; Gibson, H. W. *Org. Lett.* **1999**, *1*, 47–50.
7. Jeong, K.-S.; Choi, J. S.; Chang, S. Y.; Chang, H.-Y. *Angew. Chem., Int. Ed.* **2000**, *39*, 1692–1695.
8. Philp, J. F.; Stoddart, J. F. *Synlett* **1991**, 445–458.
9. Vögtle, F.; Händel, M.; Meier, S.; Ottens-Hildebrandt, S.; Ott, F.; Schmidt, T. *Liebigs Ann.* **1995**, 739–743.
10. Händel, M.; Plevoets, M.; Gestermann, S.; Vögtle, F. *Angew. Chem., Int. Ed. Engl.* **1997**, *36*, 1199–1201.
11. Hübner, G. M.; Gläser, J.; Seel, C.; Vögtle, F. *Angew. Chem., Int. Ed. Engl.* **1999**, *38*, 383–386.
12. Reuter, C.; Wienand, W.; Hübner, G. M.; Seel, C.; Vögtle, F. *Chem. Eur. J.* **1999**, *5*, 2692–2697.
13. Seel, C.; Vögtle, F. *Chem. Eur. J.* **2000**, *6*, 21–24.
14. Shukla, R.; Kida, T.; Smith, B. D. *Org. Lett.* **2000**, *2*, 3039–3248. Mahoney, J. M.; Beatty, A. M.; Smith, B. D. *J. Am. Chem. Soc.* **2001**, *123*, 5847–5848.
15. Deetz, M. J.; Shang, M.; Smith, B. D. *J. Am. Chem. Soc.* **2000**, *122*, 6201–6207.
16. Shukla, R.; Deetz, M. J.; Smith, B. D. *Chem. Commun.* **2000**, 2397–2398.
17. Hughes, M. P.; Smith, B. D. *J. Org. Chem.* **1997**, *62*, 4492–4501.
18. Izatt, R. M.; Pawlak, K.; Bradshaw, J. S.; Bruening, R. L. *Chem. Rev.* **1991**, *91*, 1721–2085.
19. Fyfe, M. C. T.; Glink, P. T.; Menzer, S.; Stoddart, J. F.; White, A. J. P.; Williams, D. J. *Angew. Chem., Int. Ed.* **1997**, *36*, 2068–2070.
20. Pons, M.; Millet, O. *Prog. Nucl. Magn. Reson. Spectrosc.* **2001**, *38*, 267–324.
21 Ngola, S. M.; Kearney, P. C.; Mecozzi, S.; Russell, K.; Dougherty, D. A. *J. Am. Chem. Soc.* **1999**, *121*, 1192–1201.
22. Sauvage, J.-P. *Acc. Chem. Res.* **1998**, *31*, 611–619.
23. Balzani, V.; Credi, A.; Raymo, F. M.; Stoddart, J. F. *Angew. Chem., Int. Ed.* **2000**, *39*, 3348–3391.
24. Brouwer, A. M.; Frochot, C.; Gatti, F. G.; Leigh, D. A.; Mottier, L.; Paolucci, F.; Roffia, S.; Wirpel, G. W. H. *Science* **2001**, *291*, 2124–2128.
25. Wong, E. W.; Collier, C. P.; Belohradsky, M.; Raymo, F. M.; Stoddart, J. F.; Heath, J. R. *J. Am. Chem. Soc.* **2000**, *122*, 8531–8540.
26. Anelli, P.; Spencer, N.; Stoddart, J. F. *J. Am. Chem. Soc.* **1991**, *113*, 5131–5133.
27. Asakawa, M.; Ashton, P. R.; Iqbal, S.; Stoddart, J. F.; Tinker, N. D.; White, A. J. P.; Williams, D. *J. Chem. Commun.* **1996**, 483–486.
28. Asakawa, M.; Iqbal, S.; Stoddart, J. F.; Tinker, N. D. *Angew. Chem., Int. Ed.* **1996**, *35*, 976–978.
29. Amabilino, D. B.; Dietrich-Buchecker, C. O.; Livoreil, A.; Pérez-Garcia, L.; Sauvage, J.-P.; Stoddart, J. F. *J. Am. Chem. Soc.* **1997**, *119*, 12114–12124.
30. Andrievsky, A.; Ahuis, F.; Sessler, J. L.; Vögtle, F.; Gudat, D.; Moini, M. *J. Am. Chem. Soc.* **1998**, *120*, 9712–9713.
31. Montalti, M.; Prodi, L. *Chem. Commun.* **1998**, 1461–1462.
32. Balzani, V.; Credi, A.; Langford, S. J.; Raymo, F. M.; Stoddart, J. F.; Venturi, M. *J. Am. Chem. Soc.* **2000**, *122*, 3542–3543.
33. Raymo, F. M.; Stoddart, J. F. *Chem. Rev.* **1999**, *99*, 1643–1663.
34. Parham, A. H.; Schmieder, R.; Vögtle, F. *Synlett* **1999**, *12*, 1887–1890.
35. Shigekawa, H.; Miyake, K.; Sumaoka, J.; Harada, A.; Komiyama, M. *J. Am. Chem. Soc.* **2000**, *122*, 5411–5412.
36. Bard, A. J. *Chem. Eng. News* **1999**, *77*, 5.
37. Funk and Wagnalls New International Dictionary of the English Language, World Publishing: Chicago, Comprehensive Ed., 1995, p 762.